

NJC

Accepted Manuscript



This is an *Accepted Manuscript*, which has been through the Royal Society of Chemistry peer review process and has been accepted for publication.

Accepted Manuscripts are published online shortly after acceptance, before technical editing, formatting and proof reading. Using this free service, authors can make their results available to the community, in citable form, before we publish the edited article. We will replace this *Accepted Manuscript* with the edited and formatted *Advance Article* as soon as it is available.

You can find more information about *Accepted Manuscripts* in the [Information for Authors](#).

Please note that technical editing may introduce minor changes to the text and/or graphics, which may alter content. The journal's standard [Terms & Conditions](#) and the [Ethical guidelines](#) still apply. In no event shall the Royal Society of Chemistry be held responsible for any errors or omissions in this *Accepted Manuscript* or any consequences arising from the use of any information it contains.



Journal Name

ARTICLE

Green preparation of novel heptafluoro-zirconate/hafnate nanocrystals at ambient temperature

Xianghong He,^{*a} Jinxin Cao^a and Ziyi Hu^a

Received 00th January 20xx,
Accepted 00th January 20xx

DOI: 10.1039/x0xx00000x

www.rsc.org/

Fabrication of polynary fluoride nanocrystals (NCs) at ambient temperature is a well-known challenge, since heating is generally required to produce crystallized nanomaterials. Herein we report a convenient solution-phase strategy, namely, complex chemical route, for producing pure and doped heptafluoro-zirconate/hafnate NCs under ambient conditions. The production of nanocrystals is highly dependent on the chelating agent, the feed ratio of oleic acid to Zr^{4+} , and the feed ratio of F^- to Zr^{4+} . The functionalization of these NCs by means of doping strategy was also achieved at ambient temperature. Down-shifting and up-converting fluorescence has been realized in these zirconium-/hafnium-based matrices. The proposed method of Zr^{4+}/Hf^{4+} -containing fluorides preparation is simple, efficient, cheap and easy to mass production, which might open up a new way for synthesis of polynary fluorides.

Introduction

Preparation of nanomaterial is the base for its subsequent investigation involving structure, properties and application.¹ Over the last decades, significant efforts have been dedicated to developing strategies for synthesis of 3d/4d/4f metal fluoride nanoparticles with controlled phase, shape, size, and chemical composition.² The popular techniques for the synthesis of metal fluoride nanoparticles can be classified into three categories, namely, high temperature co-precipitation,^{2h} thermal decomposition of metal trifluoroacetate precursors,²ⁱ and hydro-/solvo-thermal technique.^{2d,2i-2k,3} Although good control over phase, shape, size, and composition of fluoride nanocrystals (NCs) can be achieved in these methods, the pyrolysis of metal trifluoroacetates produces very toxic fluorinated and oxyfluorinated carbon species, which always raises some safety concerns.^{2h,2i} Moreover, these approaches also suffer from problems including complicated experimental conditions, tedious procedures, and high reaction temperatures (for example, usually exceeding 300 °C for the former, ≥ 280 °C for the latter, and ≥ 180 °C for the hydro-/solvo-thermal).^{2a,2c,2j,2k} In general, beyond obvious energetic concerns, a high temperature required for these routes is also a major barrier to the implementation of large-scale reproduction of NCs.⁴ Hence, the development of a facile room-temperature (RT) solution-phase process to fabricate pure-phase fluoride-based NCs is eagerly demanded from safety and energy-saving standpoints.^{2f,5}

To the best of our knowledge, Zr^{4+} and Hf^{4+} own the same

electronic configurations as those of rare-earth Y^{3+} and Lu^{3+} , respectively. Furthermore, they also exhibit the lanthanide contraction phenomenon and their ion radii are similar to those of heavy lanthanide ions. Consequently, Zr^{4+}/Hf^{4+} -containing fluorides can provide excellent platforms for the incorporation of a broad range of photo-active lanthanide ions.⁶ However, a synthesis procedure which allows the production of pure-phase Zr^{4+}/Hf^{4+} -containing nanocrystallines under ambient conditions has not been reported up to now.

Herein, pure and doped A_3MF_7 ($A=Na, K, M=Zr, Hf$) NCs have been successfully prepared via a convenient complex chemical procedure at RT using oleic acid as chelating agent. Against the general preconceived idea that heating is required to produce crystallized nanomaterials and for doping,⁷ the novelty of this work relies on the feasibility to prepare, under RT conditions, heptafluoro-zirconate/hafnate NCs. Moreover, we highlight that the substantial incorporation of dopant can be achieved under ambient conditions.

Experimental

Materials

Oleic acid (OA), sodium oleate (NaOA) potassium oleate (KOA), and oleylamine (OM) were purchased from Alfa Aesar Co., China. $ZrOCl_2 \cdot 8H_2O$ ($\geq 99.0\%$), $HfOCl_2 \cdot 8H_2O$ ($\geq 98.0\%$), NaF ($\geq 99.0\%$), $KF \cdot 2H_2O$ ($\geq 99.0\%$), NH_4F ($\geq 96.0\%$), rare-earths oxides (Eu_2O_3 , Yb_2O_3 , Er_2O_3 , 99.99%), concentrated nitric acid (HNO_3 , $\geq 68.0\%$), NaOH ($\geq 96\%$), KOH ($\geq 85.0\%$), ethanol ($\geq 99.7\%$), and cyclohexane ($\geq 99.5\%$) were supplied by Sinopharm Chemical Reagent Co., China. Rare-earths oxides were separately dissolved in dilute HNO_3 solution and the residual HNO_3 was removed by heating and evaporation, resulting in the formation of aqueous solution of corresponding $RE(NO_3)_3$.

^a School of Chemistry and Environmental Engineering, Jiangsu University of Technology, Changzhou, Jiangsu 213001, China. E-mail address: hexh@jsut.edu.cn

[†] Electronic Supplementary Information (ESI) available: Fig.S1–S2. See DOI: 10.1039/x0xx00000x

ARTICLE

Journal Name

Synthesis

The solvothermal procedure of K_3ZrF_7 nanocrystalline

K_3ZrF_7 nanocrystalline were synthesized by a solvothermal method. In a typical preparation, KOA (2.62 g), 5.0 mL OM, and 20.00 g OA were mixed together in a plastic beaker under stirring at room-temperature, followed by the addition of 40.00 mL alcohol solution of $ZrOCl_2$ (12.5 mM). The mixture was stirred vigorously for 2 hours. Subsequently, the aqueous solution of KF (0.19 g) and NH_4F (4.00 mL, 1.00 M) was slowly added into the mixture. After continually stirring for 30 min, the resultant mixing solution was then transferred into a 100 mL Teflon-lined autoclave. The autoclave was then placed in a digital temperature-controlled oven and operated at 50–200 °C for 12 hrs and then was allowed to cool to room-temperature naturally. Subsequently, the as-obtained nanocrystals were collected by centrifugation at 13,000 rpm, washed sequentially with cyclohexane and ethanol for several times. After drying at 50 °C under dynamic vacuum for 24 hrs, K_3ZrF_7 powder was obtained. The production yield is 89.4%.

The procedure for synthesis of A_3MF_7 ($A=Na, K, M=Zr, Hf$) NCs at RT

A_3MF_7 ($A=Na, K, M=Zr, Hf$) NCs were prepared through a solution-phase complex method at RT (25 °C). Herein took the synthesis of Na_3ZrF_7 NC as an example. In a typical preparation, 2.47 g NaOA, 5.0 mL OM, and 20.00 g oleic acid were mixed together under stirring at RT, followed by the addition of 40.00 mL alcohol solution containing 0.33 g $ZrOCl_2 \cdot 8H_2O$. The mixture was stirred vigorously for 6 hours. Subsequently, the aqueous solution of NaF (0.10 g) and NH_4F (4.67 mL, 1.00 M) was slowly added into the mixture. After continually stirring for 30 min, the mixture was left to stand for 12 hours at 25 °C. The products were collected by centrifugation, washed sequentially with cyclohexane and ethanol for several times. After dried in a vacuum at RT for 24 hours, Na_3ZrF_7 powder was obtained. The production yield is 83.1%. When NaOA was replaced by NaOH, Na_3ZrF_7 NC can be successfully fabricated.

The synthetic procedure of lanthanide-doped A_3MF_7 ($A=Na, K, M=Zr, Hf$) NCs was the same as that used to prepare Na_3ZrF_7 host, except that the stoichiometric amounts of $ZrOCl_2/HfOCl_2$ and $RE(NO_3)_3$ ($RE = Eu^{3+}, Yb^{3+}, Er^{3+}$) mixed solutions were added into the initial mixture.

Characterization

The crystallographic structure and phase purity were determined by powder X-ray diffraction (XRD) using a Japan Rigaku D-max 2500 diffractometer with Ni filtered Cu K_α radiation ($\lambda = 1.5406 \text{ \AA}$) at a voltage of 40 kV and a current of 40 mA. The morphology of the samples were characterized on a Hitachi S4800 field-emission scanning electron microscope (FE-SEM). Photo-luminescence (PL) excitation and emission spectra were obtained on an Edinburgh Instruments FLS920 spectrofluorimeter equipped with a continuous 450 W xenon lamp as excitation source. Fourier transform infrared (FT-IR) in transmission mode was measured on a Nicolet IR-200 FT-IR spectrophotometer using the KBr pellet technique.

Results and discussion

The idea of this work was inspired by our initial attempts to fabricate K_3ZrF_7 nanocrystallines via a solvothermal method. Various treatment temperatures including 130, 150, 180, and 200 °C, were utilized to fabricate pure-phase nanocrystallines. As expected, the as-obtained products belonged to K_3ZrF_7 nanoparticles shown in Fig. 1, which intrigues our further interest in the synthesis of K_3ZrF_7 NCs under lower temperature. Even if the treatment temperature reached as lower as 50 °C, the as-synthesized samples unambiguously remained pure cubic NCs. This interesting finding stimulated us to investigate the ambient temperature synthesis of heptafluoro-zirconate/hafnate nanocrystallines.

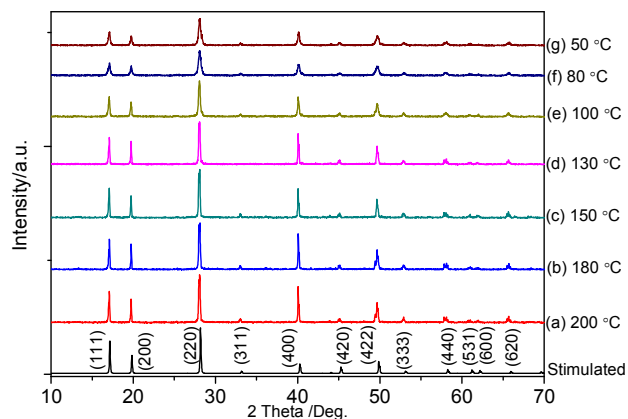


Fig. 1 XRD patterns of K_3ZrF_7 NCs obtained at various temperatures: a) 200, b) 180, c) 150, d) 130, e) 100, f) 80, g) 50 °C.

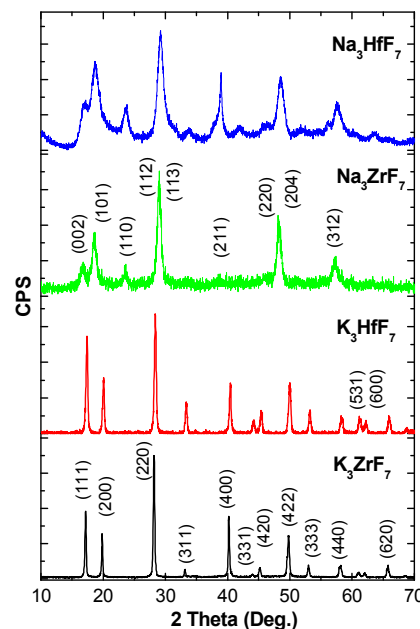


Fig. 2 XRD patterns of as-obtained K_3ZrF_7 , K_3HfF_7 , Na_3ZrF_7 , and Na_3HfF_7 NCs (background uncorrected).

A_3MF_7 ($A=Na, K, M=Zr, Hf$) NCs were synthesized by the RT reactions of A^+ and $ZrOCl_2/HfOCl_2$ with F^- in a mixture of OA, alcohol, OM, and appropriate amount of water. As shown in Fig. 2,

X-ray diffraction (XRD) patterns of heptafluoro-zirconate/hafnate samples exhibit sharp and intense peaks indicative of highly crystalline and can be well indexed as pure cubic K_3ZrF_7 (JCPDS no. 73-1530, space group $Fm-3m$), and K_3HfF_7 (JCPDS no. 78-1827, space group $Fm-3m$), tetragonal Na_3ZrF_7 (JCPDS no. 74-0808, space group $I4/mmm$), and Na_3HfF_7 (JCPDS no. 74-0809, space group $I4/mmm$), respectively. No trace of other characteristic peaks was observed for impurity phases. The calculated lattice constants are as follows: $a = b = 5.311(3)$ and $c = 10.503(2)$ Å for Na_3ZrF_7 , $a = b = 5.309(2)$ and $c = 10.500(3)$ Å for Na_3HfF_7 , $a = 8.951(1)$ Å for K_3ZrF_7 , and $a = 8.973(4)$ Å for K_3HfF_7 , which are in good agreement with the corresponding standard values for bulk tetragonal Na_3MF_7 and cubic K_3MF_7 ($M = \text{Zr}, \text{Hf}$), respectively. SEM images show that A_3MF_7 ($A = \text{Na}, \text{K}, M = \text{Zr}, \text{Hf}$) nanocrystals are uniform quasi-spherical with a diameter ranging from 51 to 73 nm for K_3ZrF_7 , 45 ~ 69 nm for K_3HfF_7 , 46 ~ 90 nm for Na_3ZrF_7 , and 40 ~ 85 nm for Na_3HfF_7 (Fig. 3). Similar shape and size are supposed to result from the same crystallographic structure and same synthesis conditions. All above results confirmed that the A_3MF_7 ($A = \text{Na}, \text{K}, M = \text{Zr}, \text{Hf}$) NCs can be successfully fabricated at RT through a facile complex chemical route.

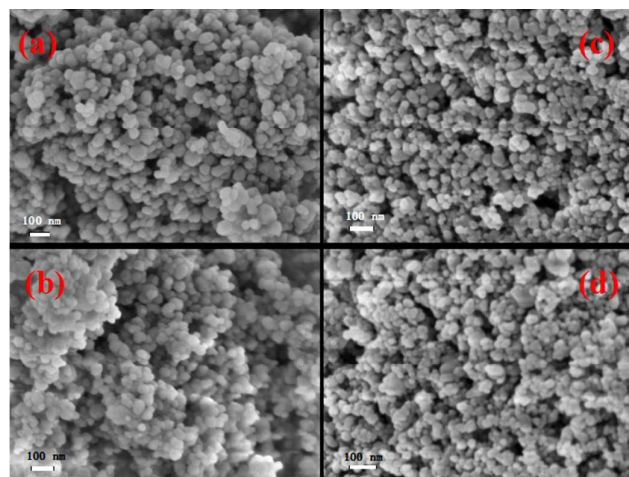


Fig. 3 FE-SEM images of (a) K_3ZrF_7 , (b) K_3HfF_7 , (c) Na_3ZrF_7 , and (d) Na_3HfF_7 NCs.

We firstly investigated the role of feed molar ratio of F^- to Zr^{4+} . The feed contents of F^- source including 5, 6, 7, 10, and 12 mmol were selected to examine the phase purity of products, while the feed amount of Zr^{4+} source and OA was fixed at 1 mmol and 60 mmol, respectively. Fig. 4 shows XRD patterns of the samples synthesized with different feed ratios of F^- to Zr^{4+} . In the case of sample which is synthesized with low content of F^- (5 or 6 mmol), a combination of cubic phase K_3ZrF_7 and KCl impurity phase was produced. When stoichiometric amount of F^- (i.e. the ratio of F^- to Zr^{4+} reached 7:1) was added into the system while other parameters were kept constant, pure-phase K_3ZrF_7 nanoparticles was obtained. Upon further increasing the content of F^- to 10 and 12 mmol, pure cubic phase potassium heptafluorozirconate compound was still obtained. The findings indicated that F^- play an important role in the formation of K_3ZrF_7 pure-phase. Apart from acting as fluorine source for K_3ZrF_7 NCs, adequate content F^- also resulted in higher crystallinity of the products.

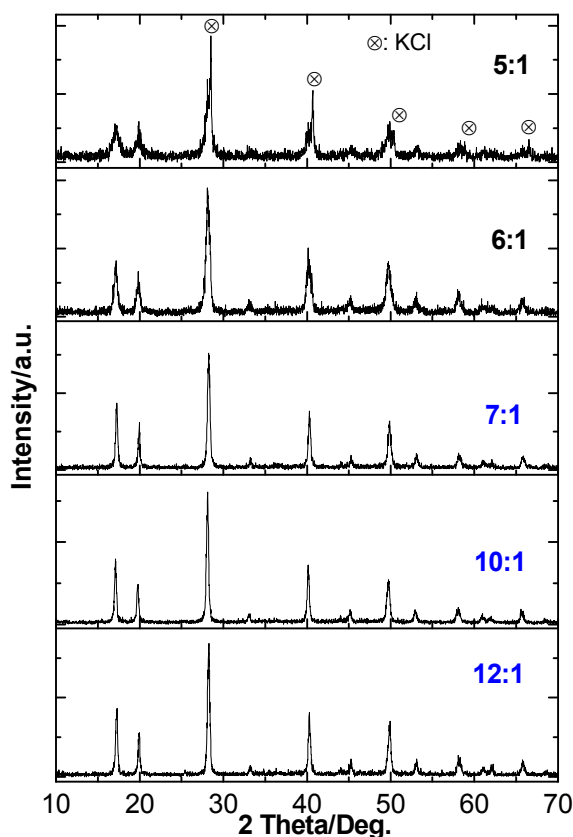


Fig. 4 XRD patterns of the as-obtained samples in the presence of different $\text{F}^-/\text{Zr}^{4+}$ feed ratio (5:1 ~ 12:1) and fixed molar ratio of OA to Zr^{4+} (60:1).

To investigate the influence of chelating agents on the formation of the pure-phase NCs, we performed the synthesis of the samples under four different chelators such as oleic acid (OA), leinoleic acid (LA), oleylamine (OM), and acetylacetone (AA). As the key assisting agent, the complexant was introduced into the reaction system to integrate all the metal ions including K^+ and Zr^{4+} ions. For comparison, we also performed the synthesis of the sample without adding any chelator. XRD patterns of the samples without and with various chelating agents are shown in Fig. 5. In the absence of any chelator, KCl and K_2ZrF_6 as impurity phases were obtained. In the case of oleylamine or acetylacetone as chelating agent K_3ZrF_7 as main phase was accompanied by KCl impurity phase. This may be due to the weak coordination force of oleylamine and acetylacetone in comparison to those of OA and leinoleic acid. When appropriate dose of OA (or leinoleic acid) was added into the reaction system, single-phase K_3ZrF_7 NCs were generated. On the other hand, OA was selected as a representative to further reveal the effect of chelating agent on the generation of pure cubic NCs. The feed amount of OA varied under the same reaction condition to get a molar ratio of OA to Zr^{4+} of 1:1, 5:1, 10:1, 30:1, and 60:1. XRD patterns of the products are depicted in Figs. 6 and 2. When the OA to Zr^{4+} ratio kept 1:1, no target phase was obtained, while two impurity phases including KCl and K_2ZrF_6 were formed. With increasing the ratio, K_3ZrF_7 as main phase was accompanied by KCl impurity phase. Once the OA to Zr^{4+} ratio

reached 30:1, single-phase K_3ZrF_7 nanoparticles was produced. With further increasing OA to Zr^{4+} ratio, the as-obtained products remained pure cubic NCs (see Fig. 2). Consequently, the presence of a certain amount of chelator is essential for the formation of phase-pure K_3ZrF_7 . The chelating agents greatly helped to mediate the production of K_3ZrF_7 NCs through the interaction between carboxylic groups and metal ions, as an indispensable medium in complex chemical process, which is similar to the role of OA for preparation of M_2NaScF_6 ($M = K, Rb, Cs$) quaternary fluoride NCs, and ultrasmall CeO_2 nanopartilces, respectively.^{5,8}

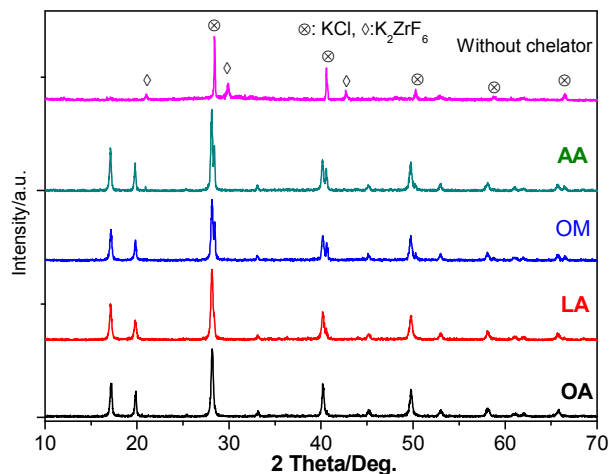


Fig. 5 XRD patterns of the products without and with various chelating agents (the molar ratio of chelating agent to Zr^{4+} remains 60:1): oleic acid (OA), linoleic acid (LA), oleylamine (OM), and acetylacetone (AA). (The impurity phases were indicated using symbols).

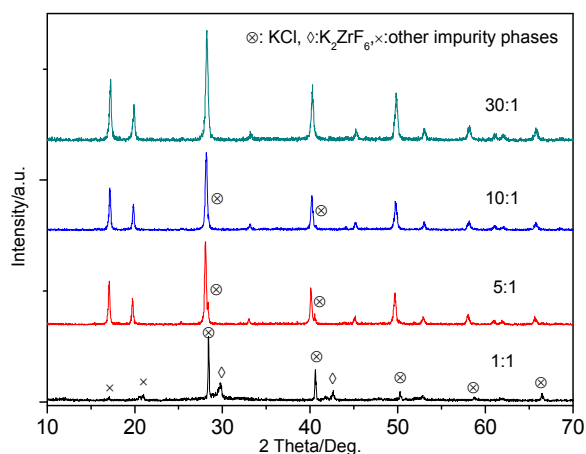


Fig. 6 XRD patterns of the samples derived at different feed ratio of OA to Zr^{4+} (1:1 ~ 30:1) in the presence of the fixed amounts of F^- and Zr^{4+} sources (The impurity phases were indicated using symbols).

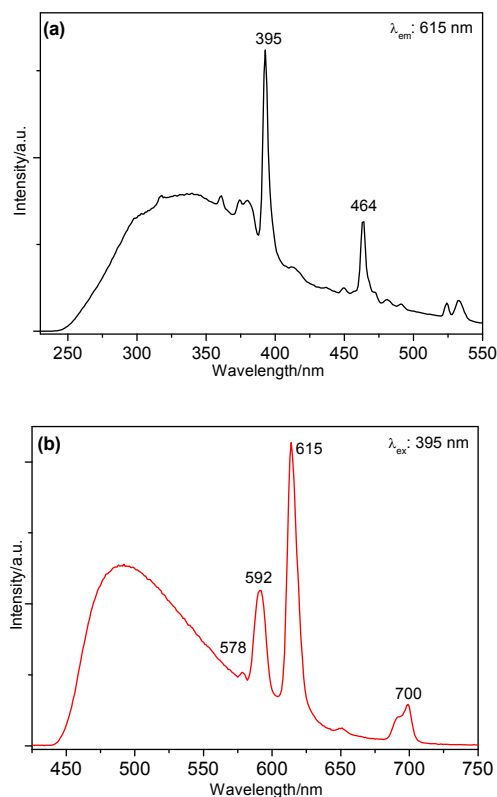


Fig. 7 RT photoluminescence excitation (a) and emission (b) spectra of $K_3ZrF_7:Eu^{3+}$ (5 mol%) NCs.

In aim to examine the feasibility of the as-obtained K_3ZrF_7 as efficient host materials, doping with Eu^{3+} and $Yb^{3+}-Er^{3+}$ was conducted under experimental conditions identical with those employed for host samples. Eu^{3+} is an excellent spectral probe to investigate the local crystal field in host lattices.^{5,9} Hence, we chose Eu^{3+} -doped K_3ZrF_7 NCs as an example to reveal whether these lanthanide ions have been successfully doped into host lattice. Fig. 7 depicts the RT excitation and emission spectra of the $K_3ZrF_7:Eu^{3+}$ (5 mol%) solid samples. Under UV irradiation, Eu^{3+} -doped K_3ZrF_7 NCs exhibits blue-greenish luminescence. The CIE coordinates for the emission spectra are calculated to be ($x = 0.3272$, $y = 0.4272$). As shown in Fig. 7a, the excitation spectrum of $K_3ZrF_7:Eu^{3+}$ is composed of a broad band centered at 340 nm, and several sharp lines between 360 and 500 nm. The sharp peaks at around 395 and 465 nm are attributed to the f-f transitions within the $Eu^{3+} 4f_6$ configuration, while the broad-band originates from defects or electronic centers caused by organic ligands adsorbed on the microcrystal surfaces.¹⁰ As shown in Fig. S1, the presence of C=O stretching band at 1706 cm^{-1} and COO^- stretching vibrations at 1659 and 1574 cm^{-1} indicates that the surfaces of NCs were capped by oleic acid molecules. It is believed that the presence of oleic acid in the reaction system resulted in the capping of as-obtained $K_3ZrF_7:Eu^{3+}$ and, hence, caused its broad band luminescence.^{2k} Upon excitation 395 nm, the emission spectrum of $K_3ZrF_7:Eu^{3+}$ consists of a broad band with a maximum at around 480 nm and intense, characteristic luminescence of Eu^{3+} ions including $^5D_0 \rightarrow ^7F_0$ at 578 nm, $^5D_0 \rightarrow ^7F_1$ at 592 nm, $^5D_0 \rightarrow ^7F_2$ at 615 nm, and $^5D_0 \rightarrow ^7F_4$ at 700 nm.

nm. The presence of a single $^5D_0 \rightarrow ^7F_0$ peak implies that Eu^{3+} ion occupies a single site in host lattices.⁹ The emission intensity of $^5D_0 \rightarrow ^7F_2$ (electric-dipole) is obviously stronger than that of $^5D_0 \rightarrow ^7F_1$ (magnetic-dipole) transition, indicating the incorporation of Eu^{3+} into a low symmetric environment.⁹ In the lattice of K_3ZrF_7 , Zr^{4+} cations are coordinated to 7 fluorine ions, resulting in $[\text{ZrF}_7]^{3-}$ pentagonal bipyramid (D_{5h}) species as isolated complex anions surrounded by K^+ ions.¹¹ The combining Eu^{3+} emission with Zr^{4+} coordination suggest that Eu^{3+} has been successfully introduced into host lattices and is occupied a low symmetry site, i.e. Zr^{4+} sites.

RT upconversion emission spectra of $\text{Yb}^{3+}\text{-Er}^{3+}$ co-activated A_3MF_7 ($\text{A}=\text{Na}, \text{K}, \text{M} = \text{Zr}, \text{Hf}$) NCs were given in Fig. S2. In comparison with $\text{Yb}^{3+}\text{-Er}^{3+}$ co-doped routine rare-earth based fluorides NCs which typically exhibit multiple-band emissions in the visible spectral region,^{2k,2l,12} a nearly single-band red emission at around 652/668 nm due to $^4F_{9/2} \rightarrow ^4I_{15/2}$ of Er^{3+} was observed, while the green emission was almost entirely restrained. The possible mechanism was presented in our most recent report.¹³

All together, the above findings revealed that A_3MF_7 ($\text{A}=\text{Na}, \text{K}, \text{M} = \text{Zr}, \text{Hf}$) can act as excellent host lattice for lanthanide ion doping.

Conclusions

In summary, we performed for the first time a systematic investigation on the ambient fabrication of heptafluoro-zirconate/-hafnate based NCs. Cubic A_3MF_7 ($\text{A}=\text{Na}, \text{K}, \text{M} = \text{Zr}, \text{Hf}$) were found to be perfect host materials for efficient emission generation of lanthanides ions Eu^{3+} and $\text{Yb}^{3+}\text{-Er}^{3+}$. This solution-phase procedure is suitable for lab-scale and industrial production of nanocrystals without high-temperature calcination or sophisticated experimental setups, and can be extended to the fabrication of other polynary fluorides.

Acknowledgements

This work has been funded by the Natural Science Foundation of China (Grant No. 21373103). J. Cao and Z. Hu would also like to thank the Practical Innovation Training Plan for the Undergraduates in Jiangsu Higher Education Institutions (No.201511463006Z).

Notes and references

- (a) S. Zhuo, J. Zhang, Y. Shi, Y. Huang, B. Zhang, *Angew. Chem. Int. Ed.*, 2015, 54, 5693; (b) H. Liu, P. Jin, Y. Xue, C. Dong, X. Li, C. Tang, X. Du, *Angew. Chem. Int. Ed.*, 2015, 54, 7051; (c) H. Duan, D. Wang, Y. Li, *Chem. Soc. Rev.*, 2015, 44, 5778; (d) J. Nai, Y. Tian, X. Guan, L. Guo, *J. Am. Chem. Soc.*, 2013, 135, 16082.
- (a) F. Wang, X. Liu, *Chem. Soc. Rev.*, 2009, 38, 976; (b) M. Haase, H. Schäfer, *Angew. Chem. Int. Ed.*, 2011, 50, 5808; (c) D. Tu, Y. Liu, H. Zhu, X. Chen, *Chem. Eur J.*, 2013, 19, 5516; (d) J. Wang, F. Wang, C. Wang, Z. Liu, X. Liu, *Angew. Chem. Int. Ed.*, 2011, 50, 10369; (e) G. Wang, Q. Peng, Y. Li, *J. Am. Chem. Soc.*, 2009, 131, 14200; (f) H. M. Zhu, C. C. Lin, W. Q. Luo, S. T. Shu, Z. G. Liu, M. Wang, J. T. Kong, E. Ma, Y. G. Cao, R. S. Liu, X. Y. Chen, *Nat. Commun.*, 2014, 5, 4312; (g) X. Ye, J. E. Collins, Y. Kang, J. Chen, D. T. N. Chen, A. G. Yodh, C. B. Murray, *Proc. Natl. Acad. Sci. USA*,

2010, 107, 22430; (h) X. Teng, Y. Zhu, W. Wei, S. Wang, J. Huang, R. Naccache, W. Hu, A. I. Y. Tok, Y. Han, Q. Zhang, Q. Fan, W. Huang, J. A. Capobianco, L. Huang, *J. Am. Chem. Soc.*, 2012, 134, 8340; (i) X. Wang, J. Zhuang, Q. Peng, Y. Li, *Nature*, 2005, 437, 121; (j) X. H. He, B. Yan, *Cryst. Growth Des.*, 2014, 14, 3257; (k) X. H. He, B. Yan, *J. Mater. Chem. C*, 2013, 1, 3910; (l) J. C. Boyer, F. Vetrone, L. A. Cuccia, J. A. Capobianco, *J. Am. Chem. Soc.*, 2006, 128, 7444.

- F. Wang, Y. Han, C. S. Lim, Y. Lu, J. Wang, J. Xu, H. Chen, C. Zhang, M. Hong, X. Liu, *Nature*, 2010, 463, 1061.
- D. V. Talapin, J. S. Lee, M. V. Kovalenko, E. V. Shevchenko, *Chem. Rev.*, 2010, 110, 389.
- X. H. He, B. Yan, *J. Mater. Chem. C*, 2014, 2, 2368.
- (a) D. Q. Chen, L. Lei, R. Zhang, A. P. Yang, J. Xu, Y. S. Wang, *Chem. Commun.*, 2012, 48, 10630; (b) R. Kasa, S. Adachi, *J. Appl. Phys.*, 2012, 112, 013506-013506-6.
- C. Andriamadianana, C. Laberty-Robert, M. T. Sougrati, S. Casale, C. Davoisne, S. Patra, F. Sauvage, *Inorg. Chem.*, 2014, 53, 10129.
- T. S. Sreeremya, K. M. Thulasi, A. Krishnan, S. Ghosh, *Ind. Eng. Chem. Res.*, 2012, 51, 318.
- (a) M. Shang, D. Geng, X. Kang, D. Yang, Y. Zhang, J. Lin, *Inorg. Chem.*, 2012, 51, 11106; (b) X. H. He, M. Y. Guan, C. Y. Zhang, T. M. Shang, N. Lian, Y. Yao, *J. Alloys Compd.*, 2011, 509, L341.
- C. Li, Z. Xu, D. Yang, Z. Cheng, Z. Hou, P. Ma, H. Lian, J. Lin, *CrystEngComm*, 2012, 14, 670.
- (a) V. Dracopoulos, J. Vagelatos, G. N. Papatheodorou, *J. Chem. Soc., Dalton Trans.*, 2001, 7, 1117; (b) M. Dova, M. Caracoché, A. Rodríguez, J. Martínez, P. Rivas, A. L. García, H. Vitorro, *Phys. Rev. B*, 1989, 40, 11258; (c) G. C. Hampson, L. Pauling, *J. Am. Chem. Soc.*, 1938, 60, 2702; (d) E. Reynhardt, J. Pratt, A. Watton, H. Petch, *J. Phys. C: Solid State Phys.*, 1981, 14, 4701.
- L. Liang, Y. Liu, C. Bu, K. Guo, W. Sun, N. Huang, T. Peng, B. Sebo, M. Pan, W. Liu, S. Guo, X. Z. Zhao, *Adv. Mater.*, 2013, 25, 2174.
- X. H. He, B. Yan, *CrystEngComm*, 2015, 17, 7169.

Table of Contents

The novelty relies in the feasibility to fabricate, under ambient conditions, pure and doped heptafluoro-zirconate/hafnate nanocrystals via a convenient complex chemical procedure.

